Band gap of InAs$_{1-x}$Sb$_x$ with native lattice constant

S. P. Svensson,[1] W. L. Sarney,[1] H. Hier,[1] Y. Lin,[2] D. Wang,[2] D. Donetsky,[2] L. Shterengas,[2] G. Kipshidze,[2] and G. Belenky[2]

[1]*US Army Research Laboratory, 2800 Powder Mill Rd., Adelphi, Maryland 20783, USA*

[2]*Department of Electrical and Computer Engineering, Stony Brook University, Stony Brook, New York 11794, USA*

The band gap energy of the alloy InAsSb has been studied as a function of composition with special emphasis on minimization of strain-induced artifacts. The films were grown by molecular beam epitaxy on GaSb substrates with compositionally graded buffer layers that were designed to produce strain-free films. The compositions were precisely determined by high-resolution x-ray diffraction. Evidence for weak, long-range, group-V ordering was detected in materials exhibiting residual strain and relaxation. In contrast, unstrained films having the nondistorted cubic form showed no evidence of group-V ordering. The photoluminescence (PL) peak positions therefore corresponds to the inherent band gap of unstrained, unrelaxed, InAsSb. PL peaks were recorded for compositions up to 46% Sb, reaching a peak wavelength of 10.3 μm, observed under low excitation at $T = 13$ K. The alloy band gap energies determined from PL maxima are described with a bowing parameter of 0.87 eV, which is significantly larger than measured for InAsSb in earlier work. The sufficiently large bowing parameter and the ability to grow the alloys without ordering allows direct band gap InAsSb to be a candidate material for low-temperature long-wavelength infrared detector applications.

I. INTRODUCTION

It has long been realized that InAsSb has the smallest direct band gap among the III–V compound semiconductors.[1] The large bowing parameter leads to a composition-dependent band gap that is considerably smaller than that of either binary end-member constituent. InAsSb as a potential material for long wavelength infrared (LWIR) detection (8–12 μm) has been discussed in the literature for decades.[2] It has met with limited success, however, primarily because the conventionally accepted range of values for the band gap bowing parameter, although large, did not predict the absorption wavelength to be adequately long at or below liquid nitrogen temperature. Also, no suitable binary substrate exists for epitaxial growth of the compositions that would be of interest.

We previously reported the development of graded buffer layers that accommodated large differences in lattice constant between GaSb and laser heterostructures.[3] This work was extended to InAsSb alloys of various compositions.[4,5] In this paper we show that the material parameters of InAsSb grown as described in Refs. 4 and 5 are intrinsic to strain-free, uniform InAsSb alloys and are not affected by strain-induced artifacts.

In the following brief review of earlier data, we equate low-temperature photoluminescence (PL) peak values with energy band gap. Using the conventional definition of the bowing parameter C we can write the band gap as

$$E_{g\,\mathrm{InAsSb}} = E_{g\,\mathrm{InSb}}x + E_{g\,\mathrm{InAs}}(1-x) - Cx(1-x), \quad (1)$$

where x is the Sb composition, and $E_{g\,\mathrm{InAs}}$ and $E_{g\,\mathrm{InSb}}$ are the energy gaps of the binary materials. Taking $E_{g\,\mathrm{InAs}} = 0.4074$ eV and $E_{g\,\mathrm{InSb}} = 0.2273$ eV at 77 K,[6] one finds that in order to reach a band gap corresponding to 10 μm at the optimal Sb composition, the bowing parameter needs to be at least $C = 0.73$ eV. Experimental data on bowing parameters were reported by Yen et al.[7] ($C = 0.6853$ eV) and by Fang et al.[8] ($C = 0.672$ eV). These were determined from 10 K PL from epitaxial InAsSb layers grown with presence of unknown amounts of residual strain and relaxation on InAs substrates.

The range of these C values, which have been accepted for a number of years, indicated that it would *not* be fruitful to pursue the bulk InAsSb alloy as a material enabling detection of light at 10 μm. Instead, various superlattice (SL) approaches such as the quantum well infrared photodetector[9] (QWIP) and the type II strained layer superlattice[10,11] (SLS) were, and continue to be, studied extensively.

The graphical compilation of band gap data by Fang et al.[8] is frequently cited. Interestingly, those authors did not include data from a second paper by Yen et al.,[12] although it was included as a reference. In that paper, published a few months after Ref. 7, Yen et al. also reported PL data from InAsSb grown on GaAs.[12] Although no bowing parameter was derived, PL peaks up to 10 μm were shown. Fitting the data from Ref. 12 yields $C = 0.83$ eV, which is significantly larger than the previously reported numbers.

The compilation by Fang et al.[8] also demonstrates a significant spread among the data points. This implies variations in the measured band gap energy for alloys of the same composition, and/or reflects inaccuracies related to the difficulty in determining the actual composition of the alloy. It may also indicate the presence of other crystal properties that affect the size of the band gap.

Ferguson et al. examined the role of phase separation in lowering the InAsSb band gap.[13] These studies involved InAsSb grown on nonlattice matched GaAs substrates and low growth temperatures deliberately chosen to induce phase separation. This resulted in phase separation into platelets of two different alloy compositions, producing a natural strained layer superlattice, similar to those grown by Kurtz et al.[14] It is well known that such SLS structures produce smaller effective band gaps than either of the constituent alloys.

Vegard's law is a consequence of the virtual crystal approximation. The basic physics that gives rise to the bowing parameter correction to the linear relationship has been treated in theoretical work since the 1960s, beginning with the development of the coherent potential approximation.[15] The underlying assumption is a perfectly random alloy. In the early

1990s atomic ordering was studied in many alloys and it was found that certain types, such as the CuPt variants, could further reduce the band gap. Wei and Zunger[16] predicted that this effect could theoretically lower the band gap in perfectly ordered InAsSb even to the semimetallic regime. Experimental observation of such band gap narrowing was claimed by Kurtz *et al.*,[14] who reported a 15 K PL peak from $InAs_{0.4}Sb_{0.6}$ at 0.132 eV, implying a $C = 0.882$ eV (our calculation). However, it does not appear that this work was followed up on. Most subsequent InAsSb work for IR detectors has been aimed at higher operating temperatures where a smaller C is sufficient to reach the entire LWIR range.[17,18]

CuPt-type ordering was observed in InAsSb by many other investigators[19,20] although no band gap energy data were presented. The question of what drives ordering in general has been discussed by, for example, Norman,[21] It is argued that the segregation of atoms with different sizes is driven by subsurface stresses induced by dimer formation. Since the InAsSb must be grown lattice mismatched to a binary substrate, residual strain is present, unless strain-relieving buffer layers are used.

The residual strain may itself change the band gap, as shown by the work of Pollak and Cardona.[22] Their derived expressions imply an increase in the band gap of $InAs_{1-x}Sb_x$ with compressive residual strains grown on GaAs, InAs, or GaSb ($x > 0.09$) and a decrease for tensile residual strains grown on InSb. Further evidence for the importance of the relaxation can be found in the work by Ferhat[23] who derived a phenomenological model for the bowing parameter that was composed of three contributions: The volume deformation, the charge exchange, and the structural relaxation. It was found that of the three, the relaxation contribution by far dominates the bowing parameter for InAsSb.

In conclusion, residual strain likely influences the accuracy of the composition values and accounts for much of the spread in earlier band gap data. Thus, the question remains unanswered of what the inherent low-temperature band gap of strain-free InAsSb, that does not exhibit ordering, is as a function of composition. Here we describe our work to produce such materials, and determine the composition with high precision, while ensuring that effects from ordering are absent.

We compared InAsSb grown with and without residual strain and investigated the degree of ordering with transmission electron microscopy (TEM) diffraction patterns. We conclude that while the mismatch strain can be important for the formation of spontaneous ordering, it is not required in order to obtain band gap energy bowing parameters in excess of 0.73 eV. The number we have derived is 0.87 eV. We claim that this parameter describes the inherent band gap of InAsSb with its native lattice constants, making InAsSb a viable materials system for low-temperature, LWIR, detector development.

II. EXPERIMENTAL METHODS

The material studied here was grown in two different Veeco solid-source molecular beam epitaxy (MBE) systems; a Gen II and a Gen-930. Both systems were equipped with As and Sb valved cracker sources. Epi-ready, exact-oriented (001) GaSb substrates from WaferTech LLC were used. The

compositionally graded 2–3.5 μm thick AlGaInSb buffer layers were designed based on principles described in the paper by Tersoff[24] and were grown at substrate temperatures ranging from 460 to 520 °C. The substrate temperature was maintained near 415 °C during the growth of the InAsSb layers. The Sb incorporation was controlled by the adjustment of the relative pressure of the group V elements as measured by beam-flux-monitors. The growth rate was about 1 μm/h. Further growth details have been presented elsewhere.[4]

$InAs_{1-x}Sb_x$ layers with x ranging from 20% to 46% were grown on GaInSb and AlGaInSb buffers. The material was characterized and the compositions of the InAsSb layers were determined with panalytical MRD high-resolution x-ray diffraction (HRXRD) systems using symmetric and asymmetric diffraction scans and reciprocal space mapping (RSM) techniques.[4,5] A discussion of the strain-free state of the InAsSb layers grown with compositionally graded buffer layers was thoroughly discussed in Refs. 4 and 5 and will not be repeated here. The PL and absorption spectra were measured with a Fourier-transform infrared (FTIR) spectrometer equipped with a liquid-nitrogen cooled HgCdTe detector with a cut-off wavelength of 14 μm. The PL was excited by either a 970 nm laser diode or a Nd:YAG laser and collected by reflective optics. Cross-sectional TEM images and electron diffraction patterns were obtained with a JEOL 2010F operated at 200 keV.

III. RESULTS AND ANALYSIS

An example of PL and absorption data are shown in Fig. 1. The absorption edge and the PL peak position coincided for all samples tested. PL could be observed up to room temperature for most samples and up to 250 K for the sample luminescing at 10 μm. The peak widths also indicated very high quality material with a 13 K full width half maximum (FWHM) of 11 meV at 10 μm (Fig. 2). This is similar[25] to the result in Ref. 14 and significantly more narrow than the data shown in Ref. 12. The FWHM in our bulk material is the same as for a GaSb/InAs SLS as seen in Fig. 2.
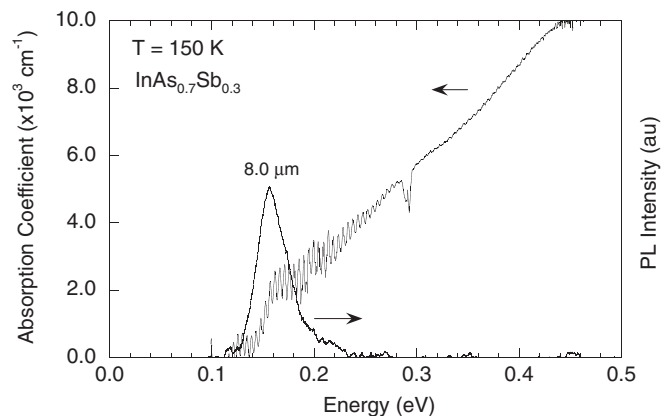

FIG. 1. Absorption and PL spectra measured at 150 K for $InAs_{0.7}Sb_{0.3}$. The PL was excited by a 970 nm laser diode at a power of 400 mW; the excitation area was 2.5×10^{-3} cm^2. The distortion near 0.29 eV was caused by CO_2 absorption.
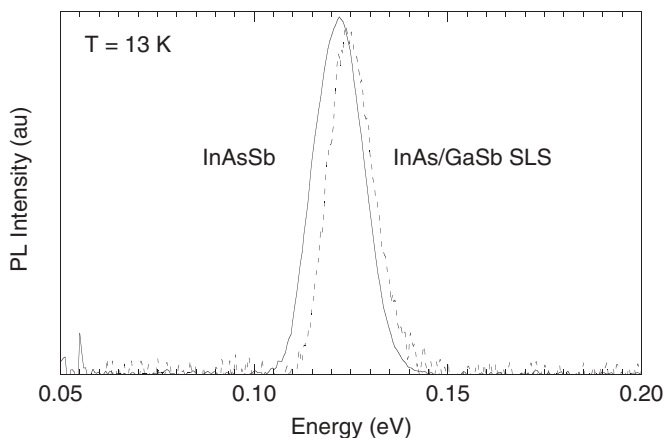
FIG. 2. PL spectra from InAs$_{0.54}$Sb$_{0.46}$ grown on an AlGaInSb buffer and from a long-wave InAs/GaSb superlattices grown on a GaSb substrate, both measured at $T = 13$ K under the same excitation of 0.1 W. The PL was excited by a Nd:YAG cw laser with a beam diameter of 0.5 mm.

The PL peak wavelengths as a function of composition are shown in Fig. 3. The data can be well fit with a parabola with $C = 0.87$ eV.

To estimate the degree of possible ordering needed to explain these observations we first use the calculations by Wei and Zunger,[16] which predicts band gaps for the 50-50 alloy of 0.18 eV and -0.28 eV for disordered vs completely ordered materials ($S = 0, 1$, where S is the ordering parameter). The functional relationship between the band gap and the ordering parameter was derived by Laks *et al.*[26] to be quadratic (see Fig. 4). This implies $S > 0.4$ in order to produce a $C > 0.87$ eV, which is a relatively high value since materials known for strong ordering, such as GaInP, typically exhibits S values below 0.6.[27]

Cross-sectional TEM samples were examined along the [110] and [$\bar{1}$10] zone axes perpendicular to the [001] growth direction. Superstructure spots due to CuPt-type ordering meet

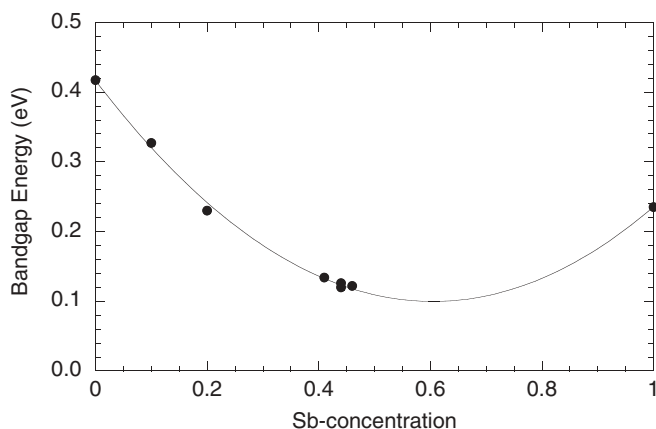FIG. 3. Energy dependence of 13 K PL maxima on composition x in InAs$_{1-x}$Sb$_x$ epitaxial layers: InAs epilayer grown on InAs substrate, InAs$_{0.9}$Sb$_{0.1}$ epilayer grown nearly lattice matched to GaSb substrate, InAsSb epilayers with $x = 0.20$ to 0.46 grown on AlGaInSb buffers on GaSb substrates. The best fit was obtained with a bowing parameter of 0.87 eV.
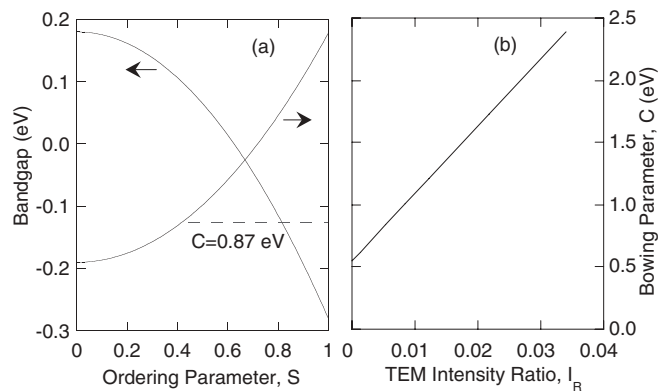

FIG. 4. The calculated relationships between (a) ordering parameter S, band gap, and bowing parameter C and (b) TEM intensity ratio I_R and bowing parameter C of InAs$_{0.5}$Sb$_{0.5}$. See text for details. The horizontal line indicates the measured bowing parameter $C = 0.87$ eV.

the visibility conditions under these imaging conditions. As an example, the [110] selected-area diffraction (SAD) pattern for the InAsSb alloy having 41% Sb (Fig. 5) show only the Bragg spots consistent with the zincblende structure of space group $T_d^2 - F\bar{4}3m$. For this zone axis, visibility conditions allow the presence of spots of $\frac{1}{2}\{\bar{1}11\}$ spots, the presence of which would indicate a doubling of the periodicity due to the ordering of As and Sb layers on the $\{\bar{1}11\}$ group V sublattice planes.

There is no such detectable presence of CuPt ordering spots in the diffraction pattern in Fig. 5, which is from a sample exhibiting 9.5 μm PL. This diffraction pattern is representative of all samples from which we are reporting PL measurements. The intensity plot in Fig. 5 shows the peaks corresponding to the periodicity of the $\{\bar{1}11\}$ planes but no extra features extending above the noise floor.

To demonstrate that TEM can observe ordering when it is present at the levels needed to affect the band gap, we examined a sample with an InAs$_{0.35}$Sb$_{0.65}$ film that was mismatched to the underlying buffer layer, and has a significant degree of residual
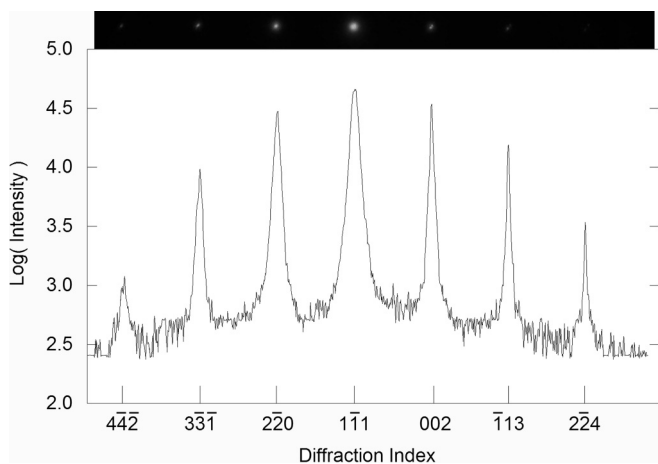

FIG. 5. TEM-SAD pattern and the intensity profile through $1\bar{1}1$ (top inset) from an InAs$_{0.59}$Sb$_{0.41}$ film showing no extra diffraction features that would indicate ordering. Ordering spots, if present, would appear halfway in between the major diffraction spots.
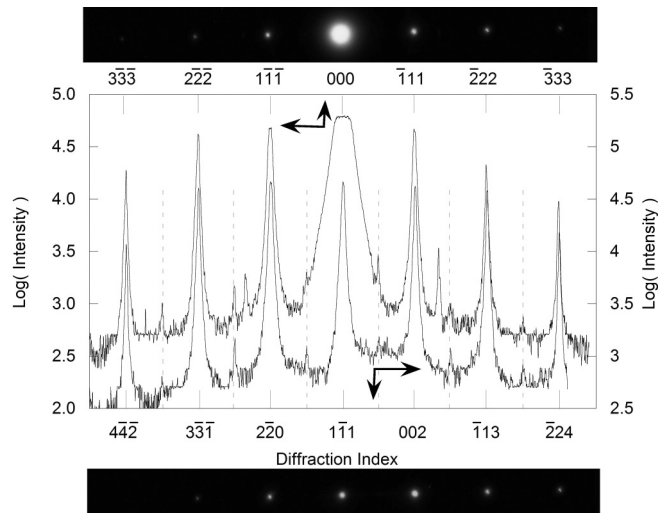
FIG. 6. TEM-SAD pattern and intensity profiles through the transmitted beam (upper inset) and through $1\bar{1}1$ (lower inset) from a strained InAs$_{0.35}$Sb$_{0.65}$ film showing extra diffraction features that indicate CuPt ordering.

FIG. 7. TEM-SAD pattern (bottom inset) and the intensity profile along (002) from a substrate rotation-induced compositional superlattice.

strain (Fig. 6). The diffraction patterns and the related intensity plots show the weak presence of superstructure spots located in between those associated with the {111} periodicity. There are also some additional features in the diffraction pattern related to the low structural quality of this particular film.

The intensities of the fundamental and superstructure spots are derived from kinematical diffraction theory using the well-known expression $I = |F_{hkl}|^2 = |\sum_i f_i e^{2\pi i(hx_1 + ky_i + lz_i)}|^2$. The detectability of ordering in TEM diffraction was estimated from the expected intensity ratio of the superstructure and fundamental spots for perfect ordering in an InAs$_{0.50}$Sb$_{0.50}$ alloy as a baseline. The intensities of the superstructure spots of $\{\frac{1}{2}\frac{\bar{1}}{2}\frac{1}{2}\}$ type, if present, relative to a $\{1\bar{1}1\}$ type spot are on the order of $I_R = S^2(f_{As} - f_{Sb})^2/(f_{As} + f_{Sb})^2$, where f_{As} and f_{Sb} are the atomic scattering factors for electrons for As and Sb as given by Edington.[28] This reduces to $I_R = \sim 0.03S^2$, leading to a linear relationship between I_R and C plotted in Fig. 4(b). We can see that the measured C value of 0.87 eV would result in an I_R of about 0.005 if ordering were inducing this level of bowing.

From Fig. 6 we can estimate a typical linear ratio between the superstructure and fundamental spots to be about 1.6 orders of magnitude. The same ratio from a regular peak to the noise floor is about 2 orders of magnitude. These numbers need to be squared to obtain the full diffraction intensity ratios. We conclude that we should be able to detect ordering greater than $S > 0.05$ (diffraction intensity at the noise floor, $I_R \sim 10^{-4}$). We estimate the degree of ordering of the sample in Fig. 6 to be $S \sim 0.13$. From Fig. 4(a) we see that ordering of this magnitude has negligible influence on the band gap energy.

This analysis is based on the case $x = 0.50$, while Fig. 5 is from a sample with $x = 0.41$. The quadratic dependence of I_R on S means that the intensity ratios are expected to drop off rapidly as an alloy becomes less ordered. This trend would be even more pronounced for alloys that do not have a 50:50 group V composition ratio. However, it reasonable to expect
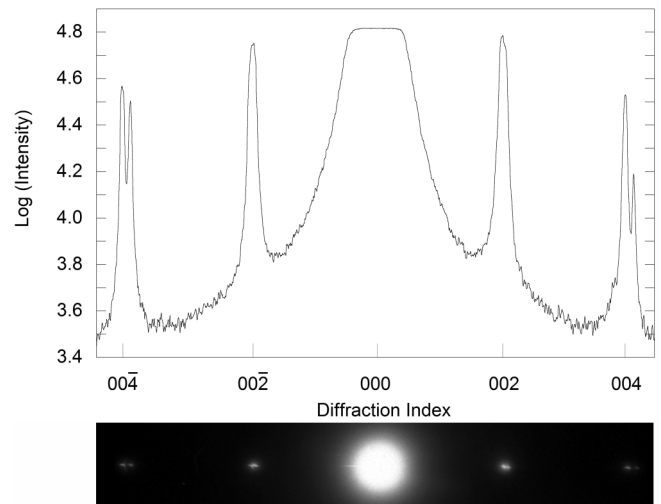
the influence of the ordering on the band gap energy to also diminish as the composition deviates from 0.50.

Artificial compositional ordering along the growth direction (001) can also be induced during MBE growth of any compound semiconductor composed of more than two elements on the different lattice sites. This originates from the source-substrate geometry and the substrate rotation used to even out thickness variations across the wafer. Unlike the parameter *thickness*, *composition* cannot be averaged at a given location in the film. Instead, at an arbitrary point at a finite radial distance from the rotation center a compositional SL may form with a band-edge amplitude that increases towards the edge of the sample.[29,30] In this study, this rotation-induced effect results in a SL of InAs$_{1-x}$Sb$_x$/InAs$_{1-y}$Sb$_y$ with a period W in Å equal to $G/R*60$, where G is the growth rate in Å/s and R is the rotation speed in revolutions per minute. The difference between x and y will increase from zero at the rotation center to larger values towards the edge. The effect must be considered here since such a SL will produce a smaller band gap than either of the x or y alloys as was demonstrated by Kurtz *et al.*[14] To minimize this effect, all samples were probed near the rotation center where the SL effect disappears. In Fig. 7 we show an example of rotation-induced ordering in a TEM sample made from an area away from the rotation center of a wafer.

These last two examples (Figs. 6 and 7) of diffraction patterns are shown as demonstrations of detectability of ordering, should it exist, and serve to underline our conclusion that the InAsSb alloys used for determining the band gap energies and bowing parameter do not exhibit ordering.

IV. CONCLUSIONS

The high-quality samples grown in this study are characterized by negligible residual strain and threading dislocation densities below ($<10^7$ cm^2) what can be detected by TEM. Ordering is absent and therefore does not influence the band gaps measured in this study, which can be described with

a bowing parameter which is significantly larger than any previously reported experimental values.

We can speculate that the reason for the absence of ordering in our samples can be due to a combination of absence of strain, the quality of the buffer layers, the use of cracker sources for the group V elements, and the quality of GaSb substrates available today.

As seen in Fig. 5 ordering may indeed be a way for the crystal to relieve residual strain.

Several other effects have previously been considered for inducing ordering. Seong *et al.*[20] studied the effect of substrate temperature during InAsSb growth and found enhanced ordering below 400 °C. Kurtz *et al.*[14] on the other hand used 425 °C and saw ordering. Our substrate temperature is in a similar range (410–415 °C). Since there can be a significant difference between temperatures quoted from different MBE machines, it is difficult to draw conclusions about the relationship between the growth temperature and the presence of ordering.

The samples examined here were all grown with cracked group V elements. Most earlier work on InAsSb, where ordering was observed, was done before Sb crackers became widely available. It is possible that the larger Sb$_4$ molecule would enhance the probability for spontaneous ordering through increased local strain.

Another way of inducing ordering is to use off-cut oriented substrates. This effect can also manifest itself as local misorientation fluctuations[31] in a substrate with less than optimum polish. The quality of GaSb and InAs substrates has consistently been lagging that of GaAs so it is not unreasonable to question the substrate quality used in many investigations 20 or more years ago and its impact on formation on ordered material.

We conclude that InAsSb with its native lattice constant and absence of ordering is a viable candidate material for low-temperature, LWIR optoelectronic device applications. It has a sufficiently small band gap, its quantum efficiency should be high owing to it being a direct band gap bulk material, and its electron and hole transport properties will not be impeded. In contrast, SLS structures for LWIR applications using the same material system tend to have issues with lower absorption coefficients[32] and poor hole transport due to the relatively large thicknesses needed in the individual layers in the SL primitive cell. (This can be partially compensated for with advanced structure designs.) These issues are mitigated for midwave designs.[33] Thus one can envision a new class of multicolor LWIR-MWIR structures consisting of LWIR bulk InAsSb materials grown on a graded buffer like the one we have used here, in combination with a MWIR SLS, strain balanced to the lattice constant of the InAsSb. This represents a reversal of strategy from previous approaches, which have sought to use bulk materials for MWIR and SLS structures for LWIR owing to the perceived lack of III–V materials with sufficiently small band gaps. It is also worth mentioning that the InAsSb alloy system lends itself ideally to implementation of White's[34] barrier-diode concept since most lattice matched combinations of InAsSb (the IR absorber layer) and AlInAsSb (the electron barrier layer) could have negligible valence band offsets that allow unimpeded minority hole transport in an *n*-type structure while providing majority electron blocking.

[1]A. G. Thompson and J. C. Wolley, Can. J. Phys. **45**, 225 (1967).

[2]See, e.g., A. Rogalski, K. Adamiec, and J. Rutkowski, eds., *Narrow-Gap Semiconductor Photodiodes* (SPIE, Bellingham, WA, 2000).

[3]G. Kipshidze, T. Hosoda, W. L. Sarney, L. Shterengas, and G. Belenky, IEEE Photon. Technol. Lett. **23**, 317 (2011).

[4]D. Wang, Y. Lin, D. Donetsky, L. Shterengas, G. Kipshidze, G. Belenky, W. L. Sarney, H. Hier, and S. P. Svensson, Proc. SPIE 8353, Infrared Technology and Applications **XXXVIII**, 835312 (2012).

[5]G. Belenky, D. Donetsky, G. Kipshidze, D. Wang, L. Shterengas, W. L. Sarney, and S. P. Svensson, Appl. Phys. Lett. **99**, 141116 (2011).

[6]I. Vurgaftman, J. R. Myer, and L. R. Ram-Mohan, J. Appl. Phys. **89**, 5815 (2000).

[7]M. Y. Yen, R. People, K. W. Wecht, and A. Y. Cho, Appl. Phys. Lett. **52**, 489 (1988).

[8]Z. M. Fang, K. Y. Ma, D. H. Jaw, R. M. Cohen, and G. B. Stringfellow, J. Appl. Phys. **67**, 7034 (1990).

[9]K. K. Choi, in *Comprehensive Semiconductor Science and Technology*, edited by P. Bhattacharya, R. Fornari, and H. Kamimura, Vol. 6 (Elsevier, Amsterdam, 2011), pp. 160–228.

[10]D. L. Smith and C. Mailhiot, J. Appl. Phys. **62**, 2545 (1987).

[11]F. Fuchs, U. Weimer, W. Pletschen, J. Schmitz, E. Ahlswede, M. Walther, J. Wagner, and P. Koidl, Appl. Phys. Lett. **71**, 3251 (1997).

[12]M. Y. Yen, R. People, and K. W. Wecht, J. Appl. Phys. **64**, 952 (1988).

[13]I. T. Ferguson, A. G. Norman, B. A. Joyce, T. Y. Seong, G. R. Booker, R. H. Thomas, C. C. Phillips, and R. A. Stradling, Appl. Phys. Lett. **59**, 3324 (1991).

[14]S. R. Kurtz, L. R. Dawson, R. M. Biefeld, D. M. Follstaedt, and B. L. Doyle, Phys. Rev. B **46**, 1909 (1992).

[15]See, for example, P. Soven, Phys. Rev. **156**, 809 (1967); J. A. Van Vechten and T. K. Bergstrasser, Phys. Rev. B **1**, 3351 (1970); M. Bugajski, A. M. Kontkiewicz, and H. Mariette, *ibid.* **28**, 7105 (1983); J. Wu, W. Shan, and W. Walukiewicz, Semicond. Sci. Technol. **17**, 860 (2002).

[16]S.-H. Wei and A. Zunger, Appl. Phys. Lett. **58**, 2684 (1991).

[17]J. D. Kim, D. Wu, J. Wojkowski, J. Piotrowski, J. Xu, and M. Razeghi, Appl. Phys. Lett. **68**, 99 (1996).

[18]Y. Z. Gao, X. Y. Gong, and T. Yamaguchi, Jpn. J. Appl. Phys. **45**, 5732 (2006).

[19]H. R. Jen, K. Y. Ma, and G. B. Stringfellow, Appl. Phys. Lett. **54**, 1144 (1989).

[20]T.-Y. Seong, G. R. Booker, A. G. Norman, and I. T. Ferguson, Appl. Phys. Lett. **64**, 3593 (1994).

[21]A. G. Norman, in *Spontaneous Ordering in Semiconductor Alloys*, edited by A. Mascarenhas (Kluwer Academic/Plenum, New York, 2002), p. 45.

[22]F. H. Pollak and M. Cardona, Phys. Rev. **171**, 816 (1968).

[23] M. Ferhat, Phys. Status Solidi B **241**, R38 (2004).

[24] T. Tersoff, Appl. Phys. Lett. **62**, 693 (1993).

[25] FWHM data is not presented in numeric form in Ref. 13. We estimate 13.5 meV from the figure. Reference 11 claims 34 meV but the graphical data appears to show ∼53 meV.

[26] D. B. Laks, S.-H. Wei, and A. Zunger, Phys. Rev. Lett. **69**, 3766 (1992).

[27] See, for example, P. Ernst, C. Geng, F. Scholz, H. Schweizer, Y. Zhang, and A. Mascarenhas, Appl. Phys. Lett. **67**, 2347 (1995).

[28] J. W. Edington, *Practical Electron Microscopy in Materials Science* (Van Nostrand Reinhold, New York, 1976).

[29] S. P. Svensson, P. N. Uppal, and D. M. Gill, J. Vac. Sci. Technol. B **14**, 2192 (1994).

[30] W. L. Sarney and S. P. Svensson, Mater. Charact. **58**, 284 (2007).

[31] See, for example, T. Suzuki, in Ref. 21.

[32] C. H. Grein, M. E. Flatté, and H. Ehrenreich, in *Proceedings of the Third International Symposium on Long-Wavelength Infrared Detectors and Arrays: Physics and Applications*, Vol. 95-28, (Electrochemical Society, Pennington, NJ, 1995), pp. 211–218.

[33] C. H. Grein (private communication).

[34] A. M. White, Infrared Detectors, US Patent No. 4,679,063 (1987).